Singular point of curves – structure, visualization and application in geometric modeling

Martina Bátorová, Pavel Chalmovianský, Barbora Pokorná, Miroslava Valíková

Abstract:

During the computations of non-linear problems such as optimization, classification of varieties in algebraic geometry, analysis of complex functions, an occurence of singular points in the area of interest plays a significant role. Singularities often appear during a qualitative change of the computed object. We consider them in case of real and complex curves as well as complex functions. We provide visualization of certain invariants arising during their description as well as elementary methods and tools used during their analysis. The covered areas form a necessary theoretical background of many application areas such as robotics, geometric modeling, computational geometry, numerical mathematics, approximation theory.

Keywords:

isolated singularity, resolution, cable knots, Riemann surface, visualization of complex function, Minkowski space-like curves.

ACM classification:

***G.1.2** [Numerical Analysis]: Approximation – Approximation of Surfaces and Contours; **G.1.5** [Numerical Analysis]: Roots of Nonlinear Equations; **I.3.5** [Computer Graphics]: Computational Geometry and Object Modeling – Curve, Surface, Solid and Object Representations; **J.6** [Computer-aided engineering]: Computer-aided design (CAD).*

1. Introduction

The idea of *regularity* is spread throughout the whole mathematics and it is a key component of many so called generic algorithms. Such algorithms work if the data are "nice" and may not work in other cases. The situation, when the data, functions or some observed aspects are not stable under arbitrary small changes of the parameters, is called *singular* or *unstable*. We consider this idea in several applications and use the visualization techniques to introduce the results to non-experts as well. The topics include singularities of complex plane algebraic curves, singularities on complex valued functions and singularities gained via intersection of real curves in Minkowski space. Due to the vast amount of results in these areas, the written examples give only a flavor of the whole field of singularities.

Intuitively, the real singularities occur on a curve, when the curve cannot be locally

approximated well by a unique tangent line. This (often) inaccurate approach has been developed into a set of theoretical tools and extended to areas where the real numbers were changed with complex numbers or even a more exotic ring, and nowadays it is used to reach far deeper than the original methods were proposed to.

The first ideas and achievements in the area of plane algebraic curves and their singularities date back to ancient Greece. However, the true beginnings of their systematic study are attributed to Newton. It was not until the centuries after his lifetime, especially the 19th one, that the rigorous methods for the investigation of singularities of algebraic curves were developed.

Today, the area of singularities of algebraic curves is a meeting point of many mathematical disciplines, both theoretical and applied. The interactions and ideas of algebraic geometry, topology, robotics, approximation theory or scientific visualizations – to mention just a few – make the subject of the singularities of plane algebraic curves a very fruitful and exciting field of study.

Singular points introduce complications not only in theory, e.g. when computing an image of a curve in a suitable map, but also in practice e.g. in numerical and scientific computations, "division by zero" etc. We wish to eliminate, to *resolve* them, which means to pass by a suitable simplification process from a singular curve to such a curve that no longer has singularities and which is still in a close connection with the original curve.

The complex analysis is well established in many branches of mathematics, like number theory or applied mathematics as well as in physics, including thermodynamics, hydrodynamics and electrical engineering.

The understanding of the function properties might be difficult, because we need 4D Euclidean space to graph a complex function of a complex variable. Several methods to overcome the need of more dimensions were developed to ease the access of the human imagination to the true image of such a function. One of them is the domain colouring method, which describes one dimension using a spectrum of colours. We used this approach in our visualization of the complex function and extended it to the 3D space. When possible, we visualized the whole domain of the function.

Cable knots are special invariants of the isolated singularities of complex curves. We briefly sketch their construction. The detailed description is far longer than this paper can comprise.

In the last topic, we show how the singularities determine the global quality of a curve in Minkowski space. In [4, 14, 5] the conditions for the control points of a quadratic and cubic planar space-like Bézier curves are looked for. We sketch the fundamental idea how to find the conditions on one specific example.

2. Plane algebraic curves and their singularities

Let $\mathbb{A}^2(\mathbb{C})$ be an affine plane over the field of complex numbers $\mathbb{C}$ and let $f \in \mathbb{C}[x, y]$, $\deg f > 0$ be a non-constant square-free polynomial in indeterminates x, y. An *affine plane algebraic curve* is the set $\mathcal{C} := \mathcal{V}(f) := \{(p_1, p_2) \in \mathbb{A}^2(\mathbb{C}) \mid f(p_1, p_2) = 0\}$. The polynomial $f \in \mathbb{C}[x, y]$ is called the *defining polynomial* of the curve $\mathcal{C}$. We define the *degree of the curve* $\mathcal{C}$ to be the degree of its defining polynomial f, i.e. $\deg \mathcal{C} := \deg f$. Intuitively, we speak about the zeros or solutions of the equation $f = 0$.

The affine plane algebraic curve $\mathcal{V}(f)$ is said to be *irreducible* iff f is irreducible, otherwise it is called *reducible*. Any reducible curve can be uniquely decomposed into a set of irreducible curves. Such a maximum irreducible algebraic subset of the curve is called an *(irreducible) component* of the curve.

The affine plane algebraic curve $\mathcal{C} \subset \mathbb{A}^2(\mathbb{C})$ consists of two types of points. The point $P \in \mathcal{C}$ is called a *singular point* of $\mathcal{C}$, if both partial derivatives $\frac{\partial f}{\partial x}, \frac{\partial f}{\partial y}$ vanish at $P = (p_1, p_2)$. A point which is not singular is called *regular*. We say that the curve $\mathcal{C}$ is *regular* if all its points

are regular, otherwise it is called *singular*.

We consider the point $P = (0,0)$. Let $f = \sum_{i=1}^{d} a_i f_i$, where homogeneous f_i have $\deg f_i = i$ and $a_i \in \mathbb{C}$ for all $i = 1, \ldots, d$. The set of tangents at singular point $P \in \mathcal{V}(f)$, the *tangent cone*, is given by the (linear) factorization of $f_i(x,y)$ with $a_i \neq 0$ and i being minimal possible. If the tangents of P are all distinct with multiplicity 1, the singularity is called *ordinary*, otherwise *non-ordinary*. Also, P is called an *i-fold* point – in particular, for $i = 2$ a *double* point, for $i = 3$ a *triple* point of given curve $\mathcal{V}(f)$ (see fig. 1).

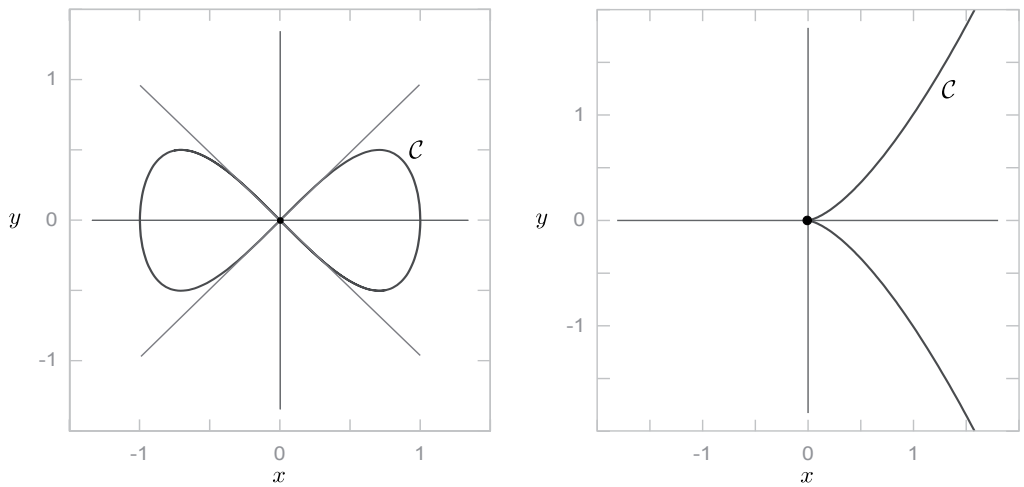

Fig. 1. Left: the origin is an ordinary double point of the Gerono lemniscate $\mathcal{C} := \mathcal{V}(x^4 - x^2 + y^2)$. The tangents at $(0,0)$ are defined by (linear) factors of $f_2(x,y) = y^2 - x^2$, i.e. as $\mathcal{V}(y-x)$ and $\mathcal{V}(y+x)$. Right: the origin is a double point of the semicubical parabola $\mathcal{C} := \mathcal{V}(y^2 - x^3)$. The double tangent at $(0,0)$ is defined by $f_2(x,y) = y^2$, i.e. as $\mathcal{V}(y)$. (Note: the figure depicts only the real part of $\mathcal{C}$).

It is convenient to consider a *projective plane algebraic curve* over the field of complex numbers i.e. the set $\mathcal{V}(F) := \{(z_0 : z_1 : z_2) \in \mathbb{P}^2(\mathbb{C}) \mid F(z_0, z_1, z_2) = 0\}$, where $F \in \mathbb{C}[z_0, z_1, z_2]$ is a homogeneous polynomial of positive degree and $\mathbb{P}^n(\mathbb{C})$ is the *projective space of dimension* n for $n \in \mathbb{N}_0$, with class of the vector $(z_0, \ldots, z_n) \in \mathbb{C}^{n+1}$ denoted by $(z_0 : \ \ldots : z_n)$.

Let $\mathcal{V}(f)$ be an affine curve and let F be the homogenization of f. The projective curve $\mathcal{V}(F)$ is called the *projectivization* of $\mathcal{V}(f)$ and $\mathcal{V}(f)$ is the *affine part* of $\mathcal{V}(F)$. We define an *affine map* $\mathcal{A}_i = \{(z_0 : z_1 : z_2) \in \mathbb{P}^2(\mathbb{C}) \mid z_i \neq 0\}$. If we homogenize f by z_0, the points of $\mathcal{V}(F)$ with $z_0 \neq 0$ correspond precisely to the original affine curve $\mathcal{V}(f)$ via $(x,y) := (\frac{z_1}{z_0}, \frac{z_2}{z_0})$. The points with $z_0 = 0$ are called the *points at infinity* of $\mathcal{V}(F)$. We define affine part and points at infinity of $\mathcal{V}(F)$ with respect to $\mathcal{A}_1, \mathcal{A}_2$ in a similar fashion.

The singularity of a point at a curve is a local property. Hence, we always consider an appropriate affine chart of the projective space. However, the global properties (such as maximum number of singular points of certain type, genus of the curve, degree and so on) have to be considered globally.

2.1 Resolution of singularities of plane algebraic curves

The process of passing from a singular algebraic curve to a curve which no longer has singularities is called a *resolution of singularities*. One of the usual resolution techniques is known as *blowup*. It enables us to find a birationally equivalent curve, which is either regular, or is less singular in a certain way. In the latter case, we can repeat the process and obtain a regular curve

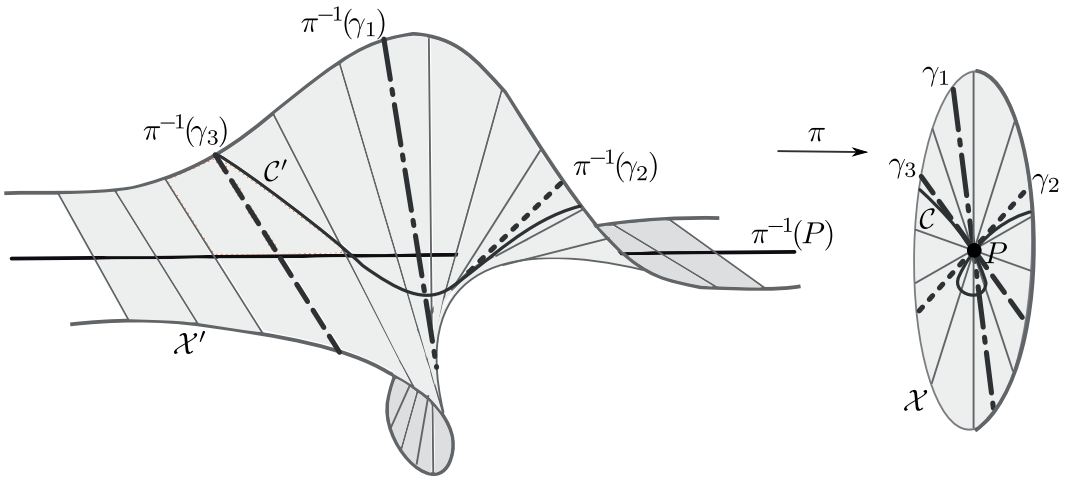

Fig. 2. The blowup of the surface $\mathcal{X}$ is a regular surface $\mathcal{X}'$. The projection $\pi\colon \mathcal{X}' \to \mathcal{X}$ is a homeomorphism of $\mathcal{X} \setminus \{P\}$, a proper mapping, and $\pi^{-1}(P)$ is the projective line $\mathbb{P}^1(\mathbb{C})$.

after a finite number of steps (see [3, 16]). However, the final curve usually lies on an algebraic surface other than the plane.

The resolution of singularity itself can be defined in general terms, but we restrict ourselves to the constructing of a resolution $\pi\colon \mathcal{C}' \to \mathcal{C}$ for which $\mathcal{C}', \mathcal{C}$ are respectively a regular curve embedded in a regular surface $\mathcal{X}'$ and a singular curve embedded in a regular surface $\mathcal{X}$; we assume that $\mathcal{X}$ lies in a projective space $\mathbb{P}^n(\mathbb{C})$ of sufficient dimension. The map π should reflect embedding of $\mathcal{C}'$ in $\mathcal{X}'$ in such a way that it corresponds to the embedding of $\mathcal{C}$ in $\mathcal{X}$, i.e. we want to construct such a curve $\mathcal{C}'$, that only the singular point $P \in \mathcal{C}$ is affected. All the other points of the neighbourhood of P remain unchanged (up to a homeomorphism), and both the curves have the same local behaviour.

The simplest case happens when $\mathcal{X} \equiv \mathbb{C}^2$ and P is an ordinary singularity of $\mathcal{C}$ placed in the origin. The essence of the blowup process then consists of replacing the point P by the set of all lines passing through P. The surface $\mathcal{X}'$ is then a ruled surface and we get a new curve $\mathcal{C}'$ (see fig. 2; for technical details see [3, 16]).

However, $\mathcal{C}$ being a planar curve is not a generic case. In general, $\mathcal{X}$ is a two-dimensional variety in $\mathbb{P}^n(\mathbb{C})$. In this situation, we use the tangent plane to $\mathcal{X}$ at P (denoted $\mathcal{T}_P(\mathcal{X})$). We construct $\mathcal{T}_P(\mathcal{X})$ by taking all tangents to curves lying on $\mathcal{X}$ and passing through P, at the point P (for more see [6]). After this, we can use the algorithm above.

The blowup of $\mathcal{X}$ is another non-singular surface $\mathcal{X}'$. Note that the fig. 2 may not give the right impression, as there is not a line through the point P but a one-dimensional projective space $\mathbb{P}^1(\mathbb{C})$, and hence (homeomorphically) a circle $\mathbb{S}^1$. The "spiral staircase" depicted is in fact an infinite Möbius strip.

In the case of complex curves, we may consider the curve as a real surface and the one we get after the resolution is a Riemann surface. We give a method of visualization for special cases of such curves in section 3..

2.2 Invariants of singularities

During the resolution, an r-fold point P is transformed into r regular points $P_1, \ldots, P_r$. This process can be visualized in the form of a *resolution tree* as follows. In the root is the original r-fold singular point P. The vertices of the first level represent points $P_{11}, \ldots, P_{1k_1}$ arising from

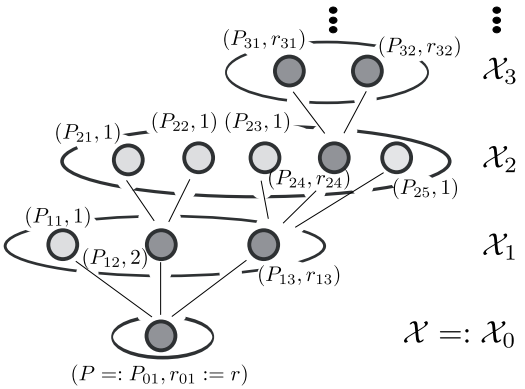

Fig. 3. An example of the resolution tree of singular curve $\mathcal{C}$ with $r_{ij} > 1$ for non-explicitly written values.

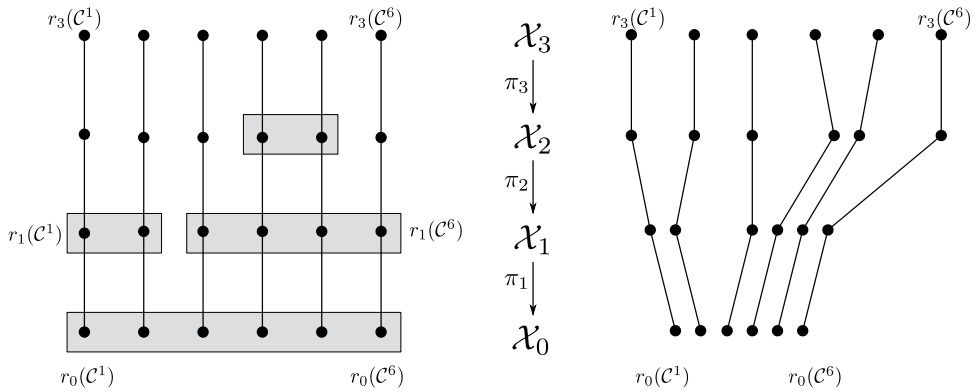

Fig. 4. A visualization of the multiplicity sequences in the case of reducible curve $\mathcal{C} = \mathcal{C}^1 \cup \ldots \cup \mathcal{C}^6$, whose resolution was obtained in 3+1 blow up steps. The separation of branches on each level is depicted either by a grey rectangle (left) or by a closeness of corresponding points (right).

the first application of blowup, along with their multiplicities $r_{11}, \ldots, r_{1k_1}$. In the second level, we blowup only singular points from the first level and depict them in a similar fashion. We continue until all arising singularities are resolved. Of course, the multiplicities at each level sum up to r (see fig. 3).

The iteration of blowups evokes subsequent changes in the internal structure of singularity. These can be reasonably encoded via the *multiplicity sequences* as follows. In the case of irreducible curves, we record the multiplicity of the point being resolved in each iteration of blowup, resulting in a finite sequence of positive integers. In the reducible case, each component is encoded in similar fashion, though we need to proceed more carefully – we write not only the multiplicities for each component, but also when the separations of branches occur. The details can be found in [3, 9, 16], for schematic depiction of multiplicity sequences see fig. 4.

The major drawback of the previous method is that we have to construct the entire resolution, which can be very tedious. Luckily, the internal structure of singularity can be characterized via *invariants*, integer values completely characterizing the structure of singularity.

The *Milnor number* μ is one of the most important invariants. I may be defined in va-

rious ways, depending whether we wish to emphasize its topological, algebraic or geometric significance. In all cases, it is the key measure of the complexity of a singularity – it can be proven, that we can break up any (isolated) singularity into μ distinct ones, each with $\mu = 1$. These singularities are very simple, each is a union of two smooth branches meeting transversely (for proofs see [16]). In case of a single branch $\mathcal{C}$, the Milnor number $\mu(\mathcal{C})$ is even, if it is smooth, $\mu(\mathcal{C}) = 0$. Another example, the *δ-invariant* of a curve, measures the number of double points of the curve.

Some numerical invariants are mutually tied, e.g. via the Plücker formulas. However, the most important result is that the topological type of $\mathcal{C}$ is completely determined by, and it determines, the system of multiplicity sequences, see [16, 9]. Thus, we may choose any of the two presented methods to describe the singularity structure, depending on the usage and available data – if necessary, they are mutually convertible.

2.3 Deformations of singularities

The technique of deformations is a fundamental method of algebraic geometry. We may deform various objects, e.g. algebraic varieties or morphisms. In our case, we use the deformations for handling isolated singularities of algebraic curves.

Loosely speaking, the deformation is a "slight change" of the curve in the neighborhood of its singularity in such a way, that the newly created curve still carries enough information about the original one. The term “slight” can be on certain examples illustrated in Euclidean topology, however for general rings it cannot be presented visually. Hence, this condition is expressed via *flatness*. Therefore, a natural question arises: is it possible to deform the curves in such a way, that the internal structure of singularity is preserved? The answer is yes.

We distinguish different types of invariant-preserving deformations, the most important are the *equimultiple*, *equinormalizable* and *equisingular* deformations. They respectively preserve the multiplicity, the δ-invariant and the Milnor number μ. In this text, we do not proceed further, the interested reader may find more in [9].

3. Riemann surface of a complex function

A notion which is very tightly bound with a complex algebraic curve is the notion of Riemann surface – a regular real two-dimensional surface obtained from the curve using resolution of singularities provided the starting curve is singular. We show the case of a complex function since any algebraic curve can be locally parameterized by such a function.

We work with the standard definition of complex numbers, the interested reader can find more in [12]. We use the compactification of $\mathbb{C}$ by a point $\infty \notin \mathbb{C}$ and the result is called *closed complex plane* $\Sigma = \mathbb{C} \cup \{\infty\}$ (see [12]). It is homeomorphic to $\mathbb{S}^2$ via stereographic projection.

We get the visualization of the closed complex plane Σ by representing the complex numbers using the two dimensional unit sphere given as equation

$$\mathbb{S}^2 = \{(x_1, x_2, x_3) \in \mathbb{R}^3 \mid x_1^2 + x_2^2 + x_3^2 = 1\}. \tag{1}$$

Identifying the Gauss plane with a plane defined by equation $x_3 = 0$ in $\mathbb{R}^3$ provides the representation of every $z = x + iy \in \mathbb{C}$ by a point with the coordinates $(x, y, 0)$. We plot the Gauss plane $\mathbb{C}$ on the unit sphere using the stereographic projection $P\colon \mathbb{C} \to \mathbb{S}^2$, which assigns point $Z = (x_1, x_2, x_3) \in \mathbb{S}^2$ to the point $z = (x, y) \in \mathbb{C}$ (see [10]). Therefore, the closed complex plane Σ is often called the Riemann sphere.

In complex analysis, we often get multivalued functions. Such a function associates with every input more than one output value (e.g. logarithm, root function). The plotting of a graph of such a function brings some problems [13]. The often used domain coloring does not give us

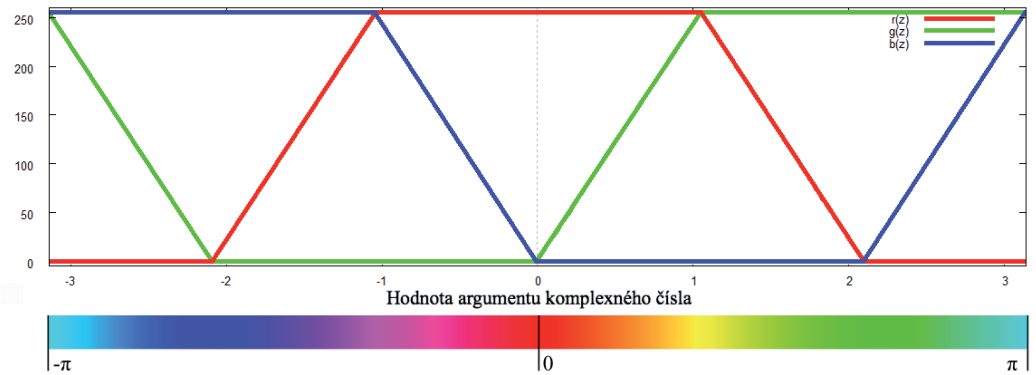

Fig. 5. The color gradient configuration used to visualize the value of the argument of a complex number in the range of $[-\pi, \pi]$. The colors changes from left to right in this order: cyan, blue, magenta, red, yellow, green, cyan. The red color shows, where the argument of the function is 0.

satisfactory results, because it plots only a part of the values of the function. Therefore, we used Riemann surface to visualize the whole family of single-valued functions which put together give the original multivalued one.

The Riemann surface is defined as a pair $(X, \mathscr{S})$, where X is a simple connected two-dimensional manifold and $\mathscr{S}$ is a complex structure on X. This structure is needed to define unambiguously the complex function $f(z)$. That means that a multivalued complex function $f(z)$ is single valued on this 2-dimensional manifold. If we take only one leaf of Riemann surface (a maximum connected subset on which the original function is uniquely defined), we get one branch of the multivalued function $f(z)$. One can find more about Riemann surfaces and their properties in [8].

3.1 Used tools and techniques

We created the visualizations using the free software `Blender`, see [2]. A user can create short scripts within the provided environment using a built-in scripting tool. The tool uses object oriented scripting language called `Python`, see [15].

In the visualization, the value of the argument is depicted via color gradient (see fig. 5). The distance of the semitransparent layer from the unit sphere is calculated using the absolute value of the function. From the definition of the absolute value, the values clearly lie in the interval $[0, \infty)$. In order to get a bounded graph, we transform the absolute value using the function $\arctan(|z|)$ (other functions are possible as well). After this transformation, we get the values from the interval $[0, \pi/2)$. Such values are used to compute the mesh of the approximated Riemann surface as several functions (represented by semitransparent layers) over the Riemann sphere. These vertices are colored according to the argument of their values.

3.2 Power function visualization

We picked the function z^n to demonstrate the proposed method. The fig. 6 illustrates the results of the script for different values of the constant $n \in \mathbb{Q}^+$. It is enough to look at the cases of positive integers and their reciprocals. In the fig. 6, we can see that for integer $n > 1$ the color gradient covers the whole Riemann sphere n-times. Hence, the values for this function of the argument are repeating. The semitransparent layer osculates with the Riemann sphere

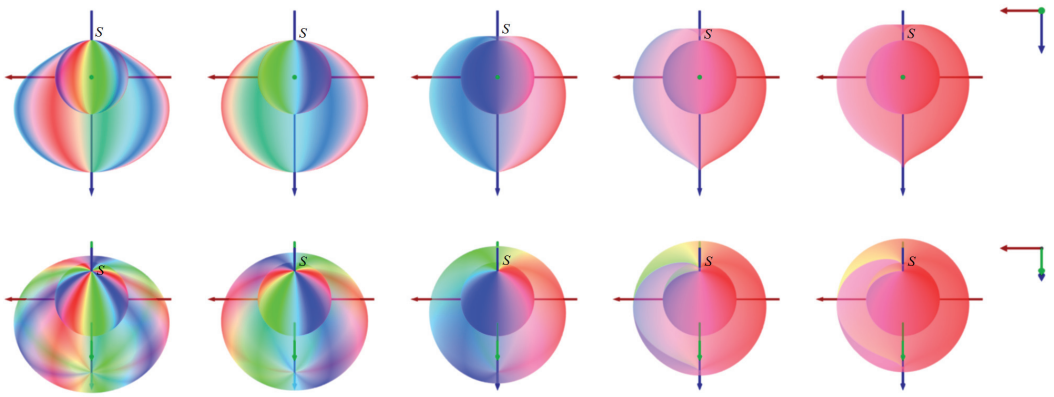

Fig. 6. The visualization of the function $z \mapsto z^n$ for values $n = 3, 2, 1, \frac{1}{2}, \frac{1}{3}$ is shown. The color gradient describes the argument of the complex number z^n. The distance of the semitransparent layer from the sphere is obtained by calculating the value of the function $\arctan(|z^n|)$. The semitransparent layer touches the Riemann sphere in the root of the polynomial.

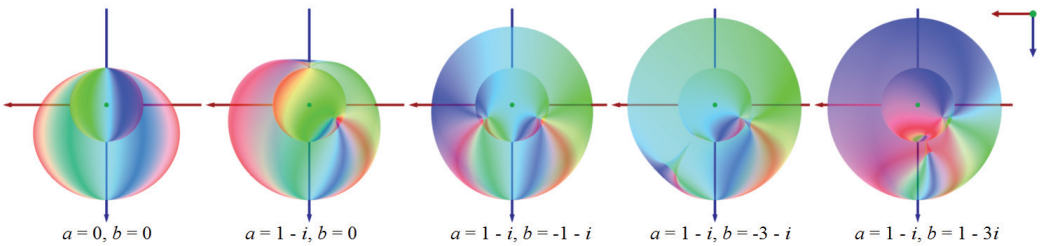

Fig. 7. In the picture, the visualization of the function $f(z) = (z - a)(z - b)$ for different values of the constants a, b is shown. Notice, the cone structures pointing to the Riemann sphere in the neighbourhood of the root of the function.

in the point S, which is the projection of the point with coordinates $(0, 0)$. The examples show the absolute values in the neighborhood of the point S are growing slower for the higher values of the exponent n and faster for the smaller values of exponent n.

For $n < 1$, there are multiple values associated with the argument, so we can see only $1/n$ of the color gradient on the Riemann sphere. This will be discussed in the subsection 3.4. In the neighbourhood of the point S the semitransparent layer has cone-like shape, which gets bigger for smaller exponent n. Hence, the absolute values of complex number are growing faster in the neighborhood of the point S.

3.3 Visualization of quadratic functions

We examined closer the function $f(z) = (z - a)(z - b)$, where $a, b \in \mathbb{C}$. In fig. 7, we see the examples for certain values of the constants a and b. Clearly, the visualization gives the graph of the function z^2 for values $a = 0, b = 0$. For different values of the constants a, b, we get two cone-like shapes formed by the semitransparent layers. These are situated in neighbourhoods of the roots of the equation $(z - a)(z - b) = 0$. It is also apparent, that the values of argument

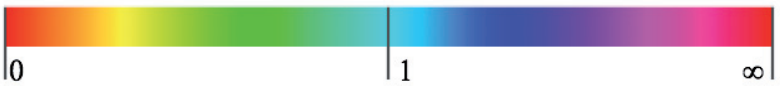

Fig. 8. The color gradient used to visualize the absolute value of the complex number. The colors change from left to right in following order: red, yellow, green, cyan, blue, magenta, red.

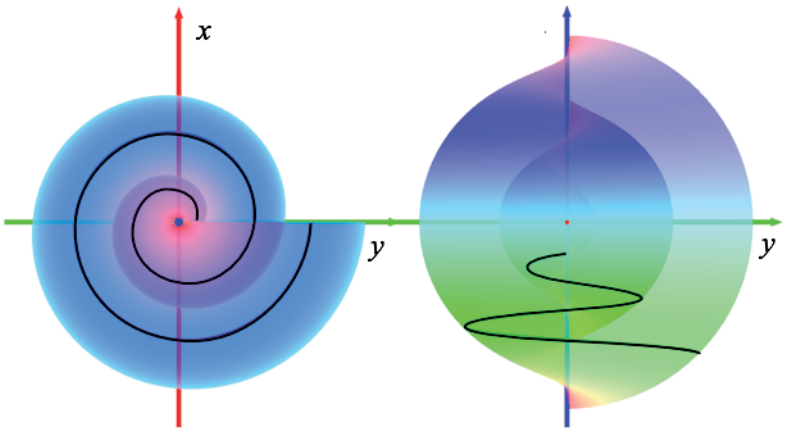

Fig. 9. The visualization of the function $f(z) = \sqrt{z}$. The viewpoint is aligned with the z-axis in the left part of the figure, the right viewpoint is aligned with the x-axis. The constant value of the modulus $r \doteq 0,4$ is highlighted.

of the complex numbers concentrate near the values of the roots.

3.4 The visualization of the Riemann surface

For obtaining the visualizations of the multivalued function using the Riemann surface, we changed the procedure of creation of the model. In this case, the absolute value of the complex number is depicted by the color gradient (see fig. 8). From the color of the point on the semi-transparent layer, we get an approximate value of the absolute value of the complex number. We highlighted the specific absolute value to get a grip for our eyes.

The value of the argument of the complex number gives us the distance from the unit sphere with the centre in the origin. This sphere represents the Riemann sphere for Σ. Hence, we get a point on the unit sphere corresponding to the zero value of the argument. If the value of the argument is π, the distance of the corresponding point on the semitransparent layer from the unit sphere is also π. In the case of multivalued function, we scale this value properly. The argument of $z = 0$ and $z = \infty$ is not defined. Therefore, we get the limit value of the argument, if it exists.

3.5 Visualization of general root function

The figure 9 represents the Riemann surface of the function $f(z) = \sqrt{z}$ using several viewpoints. In the case the viewpoint is aligned with the z-axis, the visualization produces a spiral-like shape. Therefore, the argument of the value of the function increases if we proceed counterclockwise on the circle around the branching point (a singularity).

If the viewpoint is aligned with the x-axis, the fact that the absolute value of the function increases. The graph does not contain any disruptions in the color gradient and this demonstrates the continuity of the absolute value of the function.

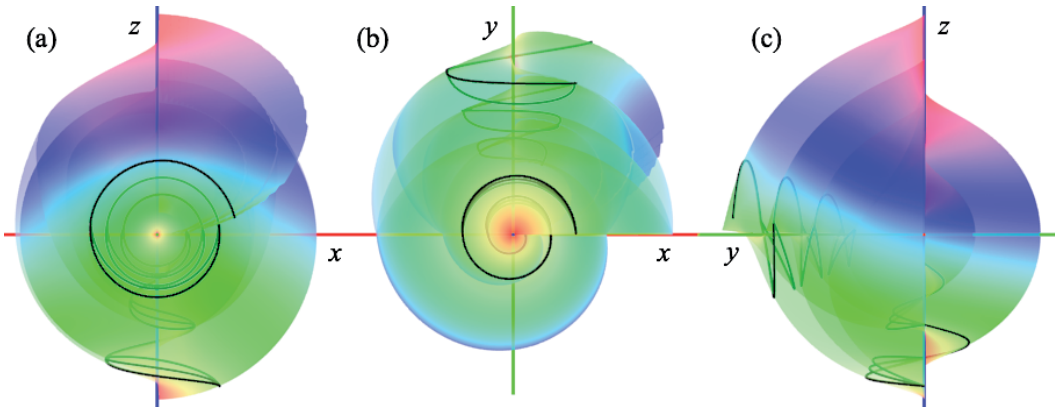

Fig. 10. Visualisation of the Riemann surface of the complex root $f(z) = \sqrt{z}\sqrt[3]{(z+i)}$ a) the viewpoint is aligned with the y-axis, b) the viewpoint is aligned with the z-axis and c) the view point is aligned with the x-axis. The images of the circles with the centers lying in the branching points $0, -i$ respectively and the radii of values $r \doteq 0,2$ respectively are depicted by the dark/black spirals. The layer intersections caused by the different degrees of the root are clearly visible in the c) subfigure.

The Riemann surface in the neighborhood of the points 0 and ∞ is in the shape of the helical surface. Therefore, these two points are the branching points of the $f(z) = \sqrt{z}$ function. The Riemann surface revolves twice around both branching points, hence the function has two branches.

A similar situation is in the case of $f(z) = \sqrt[n]{z+a}$, where the similar type of behaviour can be observed in the neighbourhood of the point $-a$ and ∞.

3.6 Visualisation of product of roots

We illustrate the general case on the function $f(z) = \sqrt[n]{(z+a)}\sqrt[n]{(z+b)}$ for $a = 0, b = i$, $m = 2, n = 3$. The fig. 10 shows the Riemann surface of the $f(z) = \sqrt{z}\sqrt[3]{(z+i)}$ function. Locally, the function is composed from two different degrees of root function. It is convenient to adapt the original function to contain only roots of the same degree, which is calculated as the least common multiple of the original degrees, resulting in the $f(z) = \sqrt[6]{z^3(z+i)^2}$ function. The visualization depicts the sixth root, therefore the final Riemann surface contains six layers. In the fig. 10, we see three double spiral around the root 0 and two triple spiral around the root $-i$. We also see the intersection of the layers between the roots. These self-intersections are caused by the used projection of the Riemann surface to the 3 dimensional space. Notice, that the function has two branch cuts. One from the branching point 0 along the half-line $l_0 = \{z \in \mathbb{R}; z \geq 0\}$ and the other from the branching point $-i$ along the half-line $l_{-i} = \{z \in \mathbb{C}; \Re(z) \geq 0, \Im(z) = -i\}$.

4. Topological classification of an isolated singularity

Each isolated singularity has in its neighborhood a stable structure given by a special knot called a cable knot.

Points in the zero set $Z(f)$, where $f(x,y) \in \mathbb{C}[x,y]$ is irreducible, $f(0,0) = 0$ and $f(0,y) \neq 0$, may be written as $(t^m, g(t)), t \in \mathbb{C}$, where $g \in \mathbb{C}\{z\}$ (the ring of complex series convergent in zero). Such a description can be considered as a parameterization of the curve using m-th root of x in a neighborhood of zero given by $y = g(x^{\frac{1}{m}})$. It is sometimes called the

Puiseux expansion of the polynomial f. The existence of such an expansion can be guaranteed using the finite algorithm via normalization process.

Minimum m allowing such a parameterization corresponds to the so called "good parameterization" of $Z(f)$. Then

$$f(x,y) = u(x,y)\prod_{j=1}^{m}(y - y(\xi^j x^{\frac{1}{m}})), \tag{2}$$

where ξ is a primitive m-th root of unity and $u \in \mathbb{C}\{x,y\}$ is a unit.

We start with a Puiseux series with mth root of x and let $E_{\mathbb{N}}$ be the set of denominators in the exponents of the Puiseux series in the terms with non-zero coefficients. Let $(m;\beta_1,\ldots,\beta_q)$ be a sequence of positive integers such that

$$\begin{aligned}\beta_1 &= \min\{k\colon a_k \in E_{\mathbb{N}}, m \nmid k\} \quad \text{and} \quad e_1 = \mathrm{GCD}(m,\beta_1),\\ \beta_i &= \min\{k\colon a_k \in E_{\mathbb{N}}, e_{i-1} \nmid k\} \quad \text{and} \quad e_i = \mathrm{GCD}(e_{i-1},\beta_i)\end{aligned}$$

for $i = 2,\ldots,g$, with $e_g = 1$, where GCD denotes the greatest common divisor. Let $e_0 = m$. This sequence is called the *Puiseux characteristics* and the sequence $\{e_0;e_1,\ldots,e_g\}$ is called the *associated Puiseux sequence*.

Example: $f(x,y) = x^3 - y^2$ with parameterization $x = t^2, y = t^3$ has the Puiseux characteristic $(2;3)$ with the associated Puiseux sequence $(2;1)$.

4.1 Knot construction

A complex algebraic curve $C \subset \mathbb{C}^2$ can be considered as a real surface in $\mathbb{R}^4 = \mathbb{C}^2$. The knot associated to a singularity is a intersection of such a surface and a small sphere around the singularity. It is known to be independent of the radius ϵ for small enough $\epsilon > 0$.

Let $K = C \cap \mathbb{S}^3_\epsilon$ be the knot associated with the singularity. A good parameterization can be obtained via projection on the cylinder $Q = \{(x,y) \in \mathbb{C}^2 : |x| = \delta\} \equiv \mathbb{S}^1 \times \mathbb{C}$ for sufficiently small $\delta > 0$.

The knot equation has the form

$$x = t^m, y = a_1 t^{\beta_1} + a_2 t^{\beta_2} + \cdots + a_g t^{\beta_g}, \tag{3}$$

where $a_1,\ldots,a_g \neq 0$ are properly picked.

By a mapping of m copies of circle with radius $\sqrt[m]{\delta}$ for x and taking corresponding y, we get the image of the knot. For $t = \sqrt[m]{\delta}e^{i\theta}, \theta \in [0,2\pi]$, we get

$$x = \delta e^{im\theta}, y = a_1 \sqrt[m]{\delta^{\beta_1}} e^{i\beta_1\theta} + a_2 \sqrt[m]{\delta^{\beta_2}} e^{i\beta_2\theta} + \cdots + a_g \sqrt[m]{\delta^{\beta_g}} e^{i\beta_g\theta} \tag{4}$$

Example: Continuing with the example of the cusp, we have the equation $y^2 = x^3$ and its parameterization after a substitution of $t = e^{i\theta}$ gives $x = e^{i2\theta}, y = e^{i3\theta}$ for $\theta \in [0,2\pi]$. The corresponding figure is in fig. 11.

In case of more complex singularities and their knots, one can use a sequence of steps for building the final knot. It can be considered as a sequence of wrapping around previously constructed knot (see the additive structure of the coordinate y in (3)).

Both coordinates are cyclic, hence it is covenient to graph them on a torus. The coordinate x is represented by parallels of the torus and the coordinate y by the meridians. In fig. 11, the meridian direction is wrapped three times while the parallel direction two times. This corresponds to the exponents in parameterization or in the Puiseux characteristic. Similarly, the meridian direction of the red knot is for the parameterization in fig 12(a) wrapped two times around the blue one while the parallel direction is wrapped 7 times. Composing together, it gives the 7 wraps around the meridians while 4 wraps around the parallel direction of the basic torus.

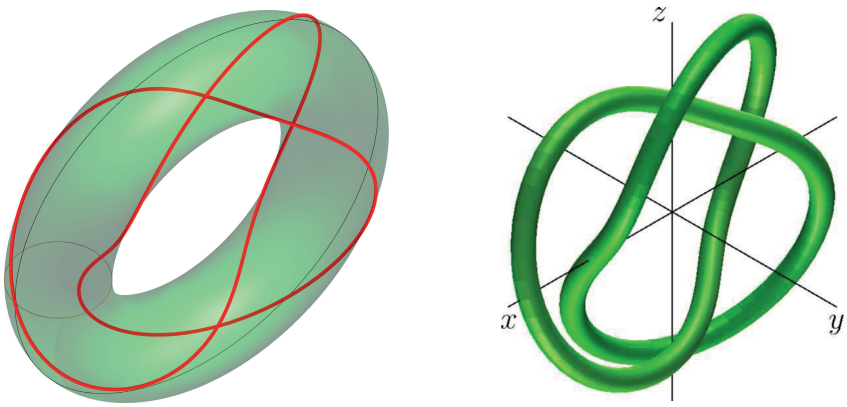

Fig. 11. The knot associated with the cusp at the curve given by the equation $x^3 - y^2 = 0$.

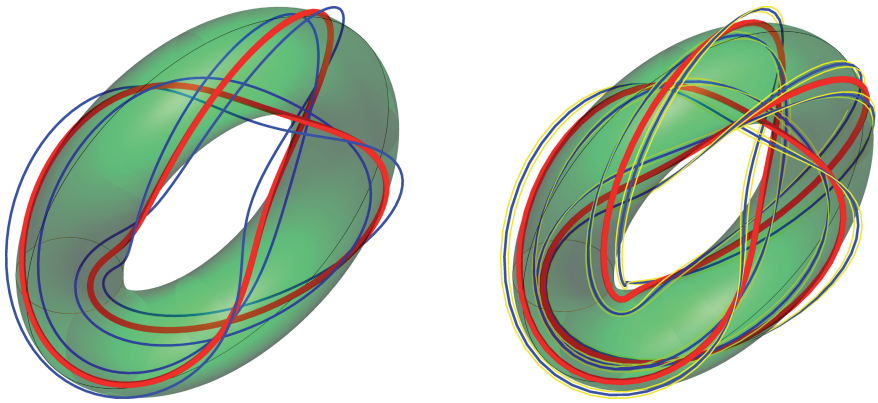

(a) (b)

Fig. 12. Examples of more complex knots in singularities with local parameterization (a) $x = e^{i4\theta}$, $y = e^{i6\theta} + e^{i7\theta}$, its Puiseux characteristic (4;6,7) and its associated Puiseux sequence (4;2,1); (b) $x = e^{i12\theta}$, $y = e^{i16\theta} + e^{i18\theta} + e^{i19\theta}$, its Puiseux characteristic (12;16,18,19) and its associated Puiseux sequence (12;4,2,1).

In general, if T_k is a torus for the first k terms in (3), adding the next term produces the knot wrapping $\frac{e_k}{e_{k+1}}$ in parallel direction and $\frac{\beta_{k+1}}{e_{k+1}}$ times wrapping in the meridian direction. Using this information, one can generate a carousel (see fig. 13) for a construction of the knot at once. One pushes the largest circle around the torus once and the other are turning with relative speed given by the numbers in Puiseux characteristic. Hence, the knot can be generated "mechanically".

5. Space-like Bézier quadratic curves in Minkowski space

The structure of real singularities is a bit more difficult to detect. We show its usage in the area of modeling in Minkowski space. Since affinely there is no difference to the Euclidean plane, the properties interesting in Minkowski space have to be determined by the (pseudo-)scalar product. We give a short overview.

Pseudo-Euclidean space, denoted by $\mathbb{R}^n_p$, $n \in \mathbb{N} = \{1, 2, 3, \dots\}$, $p \in \mathbb{N}_0 = \{0, 1, 2, \dots\}$ is

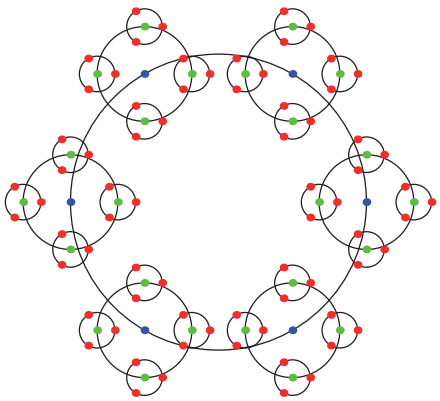

Fig. 13. Carousel and the corresponding knot for generating the characteristic knot of a singularity out of Puiseux characteristic $(72; 42, 111, 160)$ and $\mathbf{e} = (72; 6, 3, 1)$.

an n-dimensional real vector space with a regular quadratic form $\mathbf{q}\colon \mathbb{R}^n \to \mathbb{R}$, where

$$\mathbf{q}(x_1, \ldots, x_n) = \sum_{i=1}^{n-p} x_i^2 - \sum_{j=n-p+1}^{n} x_j^2$$

in a certain basis. For $p = 1$, it is called *Minkowski space*. For $p = 0$, we get *Euclidean space*. We use the notation $\overline{x} = (x_1, \ldots, x_n)^\top$ for the vectors in $\mathbb{R}_p^n$. More can be found in [1].

A quadratic form has an associated polar form P, which plays the role of scalar product. Hence, we call it the *pseudo-scalar product* since positive definiteness might not be satisfied. The vectors $\overline{x}, \overline{y} \in \mathbb{R}_p^n$ are *pseudo-orthogonal* if $P(\overline{x}, \overline{y}) = 0$.

By a standard construction, we get an affine space with a *pseudo-Cartesian* coordinate system $S(O, x_1, \ldots, x_n)$. Using the quadratic form, we classify the vectors in the pseudo-Euclidean space as follows. We call the vector $\overline{x} \in \mathbb{R}_p^n$ *space-like* if $\mathbf{q}(\overline{x}) > 0$, *time-like* if $\mathbf{q}(\overline{x}) < 0$ and *light-like* if $\mathbf{q}(\overline{x}) = 0$. All the vectors in $\mathbf{q}^{-1}(0)$ are also called *isotropic*. The set of all light-like vectors forms an *isotropic cone* Q of the corresponding quadratic form $\mathbf{q}$.

A point $x \in \mathbb{R}_p^n$ is space-like (time-like, light-like respectively) if its position vector $\overline{x} = x - O$ is such. Note that this depends on the coordinate system.

Now, there are two possible ways, how to define a space-like curve. A differentiable curve $p\colon I \to \mathbb{R}_p^n$ is called *tangentially space-like* if the tangent vector $\dot{p}(t)$ is space-like for each $t \in I$. A curve $p\colon I \to \mathbb{R}_p^n$ is called *point-wise space-like*, if it contains only space-like points, i.e. the vector $\overline{p(t)} = p(t) - O$ is space-like for every $t \in I$. In our work, we use the definition of the point-wise space-like curve. One of the advantages is that the condition of differentiability is not required, although the curves we consider in this paper are polynomial.

Bézier curve in Minkowski space of degree n is the polynomial map $b : [0, 1] \to \mathbb{R}_1^n$ that $b(t) = \sum_{i=0}^{n} B_i^n(t)\, b_i$ for $t \in [0, 1]$. Points $b_i \in \mathbb{R}_1^n$ are called control points, $B_i^n(t) = \binom{n}{i}(1-t)^{n-i}t^i$ for $i \in \{0, \ldots, n\}$ are Bernstein polynomials of degree n. More properties can be found in [7, 11].

There is an alternative way of the Bézier curve definition. Instead of one control point, we determine one point of the curve and the tangent line to the curve at this point. For the curves of degree higher than 2, the definition may be ambiguous, but it allows us to define some useful maps.

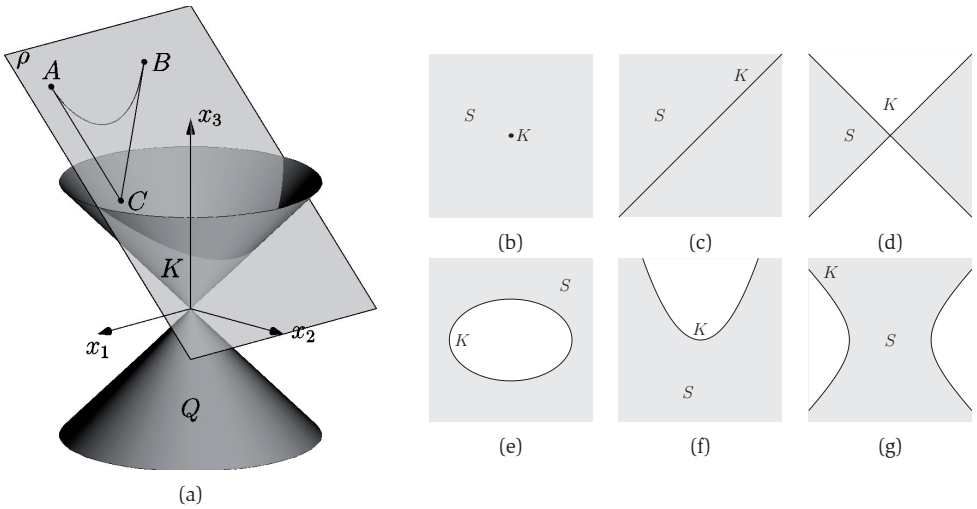

Fig. 14. (a) Plane ρ spans the points A, C, B. In the case of their non-collinearity, they generate ρ as their affine hull. The conic section K is an intersection of the light cone Q and the plane ρ.
(b–g) Let $K \subset \rho$ be the conic section (point, double line, pair of lines, ellipse, parabola, hyperbola). The set S consists of all space-like points in the plane ρ.

5.1 Space-like conditions

Let us consider Minkowski space $\mathbb{R}^3_1$ and a quadratic Bézier curve with the control points A, C, B in this order, denoted by $b_{ACB}(t)$. In order a Bézier curve to be space-like, each of its points has to be space-like. Let the points $A = [a_1, a_2, a_3]$ and $B = [b_1, b_2, b_3]$ be fixed. Since Bézier curve interpolates its endpoints, we have necessary and sufficient conditions

$$a_1^2 + a_2^2 - a_3^2 > 0, \tag{5}$$
$$b_1^2 + b_2^2 - b_3^2 > 0. \tag{6}$$

The quadratic Bézier curve is planar and it lies in the affine plane $\rho \subset \mathbb{R}^3_1$. Now, we fix the points A, B. In any case, the intersection of the light-cone Q and the plane ρ is a conic section K (see fig. 14(a)). The figures 14(b-g) show all cases of the set S of space-like points in any type of the plane ρ. The point-wise space-like Bézier curve $b_{ACB}(t) \subset S$. We solve the problem in the plane ρ for each type of conic section and the planar results can be put together to form the spatial result.

Let $S_\rho(O, x, y)$ be any pseudo-Cartesian coordinate system in the plane ρ. Let $A = [a_x, a_y], C = [c_x, c_y], B = [b_x, b_y]$ be the local affine coordinates of the control points in $S_\rho(O, x, y)$. From now on, the points A, B are arbitrary, but fixed, and they satisfy the conditions (5), (6).

Let $V_\rho(A, B)$ be the set of points $C \in \rho$ such that the curve b_{ACB} is space-like. Then, we say that $V_\rho(A, B)$ is a *set of admissible solutions* in the plane ρ with respect to A, B. If no confusion arise, we say only the set of admissible solutions V.

By $V^v_\rho(A, B)$, we denote the set of points $C \in \rho$ such that $b_{ACB} \cap K = M$, where $X \in M$ is a point of contact of order 2 between $b_{ACB}(t)$ and K. The set of points $C \in \rho$ such that b_{ACB} and K have transversal intersection is denoted by $V^t_\rho(A, B)$. The union of disjoint sets $V_\rho(A, B) \cup V^v_\rho(A, B) \cup V^t_\rho(A, B)$ gives the whole plane ρ for the given points A, B.

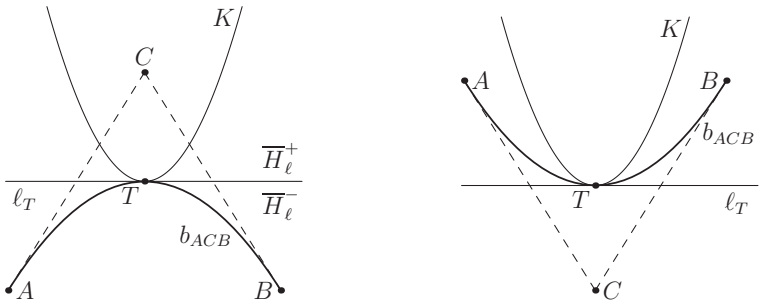

Fig. 15. Separation of the conic section K and the Bézier curve $b_{ACB}(t)$ by the tangent line ℓ_T: (a) exterior point of contact T, (b) interior point of contact T.

5.2 Set of admissible middle control points

We study the set $V_\rho^v(A,B)$. It is natural, because a "boundary" between the situation that two curves have no common points and the situation that one curve intersects the other curve is, that they touch each other in our setup.

We say that the set $D \subset K$ is the *set of points of contact* between K and the set of all b_{ACB} if for any point $X_0 = [x_0, y_0] \in D$ there is at least one point C_0 such that $C_0 \in V_\rho^v(A,B)$ and $X_0 \in b_{AC_0B} \cap K$.

We divide the points of contact into two groups. Points $T \in D$ such that the Bézier curve and the conic section K are lying in the opposite half-planes with respect to their common tangent line ℓ_T at the point T form the set of exterior points of contact D_{ext}. In the set of interior points of contact D_{in} are such points $T \in D$ that the Bézier curve and conic section K are lying in the same half-plane with respect to their common tangent line ℓ_T at the point T (see fig. 15). Clearly, $D = D_{ext} \cup D_{in}$.

Let us consider the situation that the conic section K is a unit circle and the points A, B are space-like as in fig. 16. As we proved in [14], the sets D_{ext}, D_{in} are considered with respect to the tangent lines from the points A, B to the conic section K. Let $t_{1A}, t_{2A}, t_{1B}, t_{2B}$ be the tangent lines from the points A, B to K and the points $T_{1A}, T_{2A}, T_{1B}, T_{2B} \in K$ be the corresponding points of contact.

The set $D_{ext} = \overset{\frown}{T_{1A}T_{2A}} \cap \overset{\frown}{T_{1B}T_{2B}}$, because it is the only arc on the K containing such points T that the corresponding tangent lines ℓ_T separate the Bézier curve and the conic section K. We also proved that the set D_{in} is determined by the tangent lines from A, B to K that do not separate the segment AB and K. In our case, these are t_{2A}, t_{2B}. The set $D_{in} \neq \emptyset$ iff t_{2A}, t_{2B} converge, therefore the point $P = t_{2A} \cap t_{2B}$ lies in the same half-plane with respect to line $\overleftrightarrow{AB}$ as the points t_{2A}, t_{2B}. In general, the set of interior points of contact is determined by the arc $\overset{\frown}{T_{2A}T_{2B}}$. In this case, the set D_{in} consists of two affiliated components $\overset{\frown}{T_{2A}U_1} \cup \overset{\frown}{U_2T_{2B}} \cup \{U_1, U_2\}$. The split of the arc is caused by the existence of the curve b_{AC_uB}, which has double contact with the conic section K. As one can see, $b_{AC_uB} \cap K = \{U_1, U_2\}$.

For the given points $A, B, X \in D \subseteq K$ and the tangent line ℓ_X at X to K, the Bézier curve b_{ACB} touching the conic section K is clearly identified. In order to find the middle control vertex C, we use the following map σ. The map $\sigma : D \to \rho$ is called *boundary map* if for every $X \in D$ holds $\sigma(X) = C$, for C from the definition of the set of contact points (see fig. 17). The boundary map has the form

$$\sigma(X) = \frac{b(t_0) - B_0^2(t_0)A - B_2^2(t_0)B}{B_1^2(t_0)}, \tag{7}$$

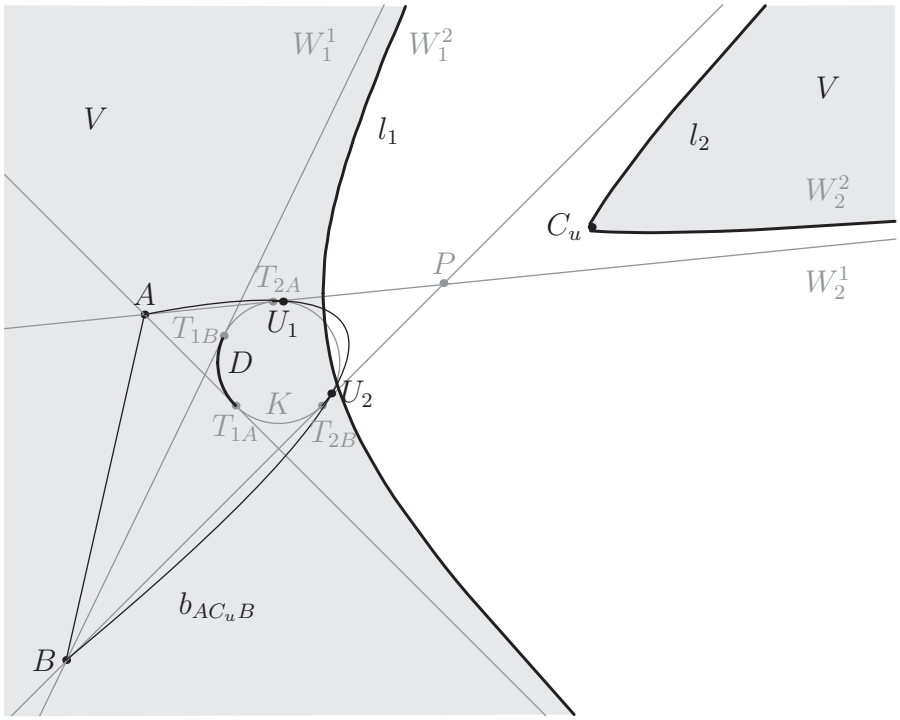

Fig. 16. Example of the set of admissible solutions $V(A, B)$ for the conic section K being a unit circle.

where $t_0 \in [0, 1]$ is a solution of the equation $0 = \alpha t_0^2 + \beta t_0 + \gamma$ and for $A = [a_x, a_y, 1]$, $B = [b_x, b_y, 1]$, $X = [x_0, y_0, 1]$ are

$$\alpha = (A - B)M_K X^\top,$$
$$\beta = 2(X - A)M_K X^\top,$$
$$\gamma = -\frac{\beta}{2}.$$

As we proved in [14], the set $V_\rho^v(A, B)$ generated by the set D using the map σ, forms the boundary ∂V of the set of admissible solutions $V(A, B)$.

In our case, the set of points of contact $D = D_{ext} \cup D_{in}$ generates the curves l_1, l_2 such that $l_1 \cup l_2 = \partial V_\rho(A, B)$, see fig. 16. Because the curve l_1 is generated by the exterior points of contact, the region W_1^1 containing the points A, B is the subset $W_1^1 \subset V_\rho(A, B)$. The curve l_2 is generated by the interior points of contact. It bounds the region W_2^2 not containing the points A, B and $W_2^2 \subset V_\rho(A, B)$ according to the theorem proved in [14]. The set of admissible solutions $V_\rho(A, B) = W_1^1 \cup W_2^2$ consists of two regions.

However, there are some specific cases in the solution for other types of conic sections. For example, the two components of hyperbola are to be considered separately and the final result is obtained as intersection of the two partial results.

6. Conclusion

We have surveyed basic notions and selected new results in the research of algebraic curves and their singularities. We have presented multiple tools and methods for measuring and capturing the internal structure of given singularities, as well as techniques for their complete removal

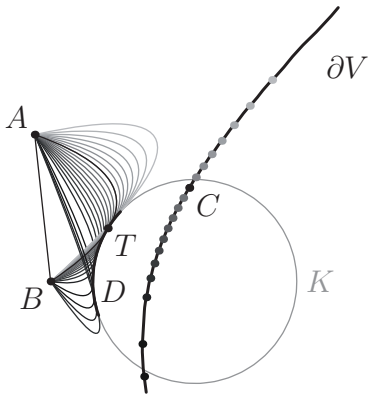

Fig. 17. The boundary map σ maps the points of the arc D to the points in ∂V. Clearly, $\sigma(T) = C$.

while preserving essential properties of the original curve. This has served as a preparation for the final topic of the text, the deformations of singularities, which enable us to study the singularities of algebraic curves and their internal structure from a different point of view.

We have also created visualizations of elementary functions over the Riemann sphere and described the generation of the Riemann surface of root functions and their product. Our approach enables to visualize all branches of a function over its domain.

A user may interact with the created 3D model, they can be edited and used for creation of animations. These features lead to a better understanding of the function behavior in both studying and tutoring sessions.

One of the aims is to use such functions for local parameterization of the algebraic curves. The isolated singularities of algebraic curves have a knot invariant describing completely the topological characteristic of the singularity. Hence, the knot can be composed out of knots of the parameterising functions.

In the future work, we want to use the deformations in order to clarify the structure of an isolated singularity and present its transition to a regular situation.

Finally, we also showed the usage of real singularities in classification of Bézier quadratic curves in Minkowski space. It is completely described in [14]. Currently, we work on the case of special higher degree Bézier curves. Some partial results are given in [5]. For example, we derive the form of the boundary map σ for cubic curves and we describe and study the problem of ambiguity of alternative definition of Bézier curve.

References

[1] M. BERGER. *Geometry I, II*. Universitext. Springer-Verlag, Berlin, 1987. Translated from the French by M. Cole and S. Levy.

[2] Blender. `http://www.blender.org/`, 2012.

[3] E. BRIESKORN and H. KNÖRRER. *Plane Algebraic Curves*. Birk-Häuser Verlag Basel, New York, 1986.

[4] P. CHALMOVIANSKÝ and B. POKORNÁ. Quadratic space-like Bézier curves in the three dimensional Minkowski space. *Proceedings of Symposium on Computer Geometry*, 20:104–110, 2011.

[5] P. CHALMOVIANSKÝ and B. POKORNÁ. Planar cubic space-like Bézier curves in the three dimensional Minkowski space. *Proceedings of Symposium on Computer Geometry*, 21:93–98, 2012.

[6] M. P. DO CARMO. *Differential Geometry of Curves and Surfaces*. Prentice Hall Inc. Englewood Cliffs, New Jersey, 1976.

[7] G. FARIN, J. HOSCHEK, and M.-S. KIM, editors. *Handbook of computer aided geometric design*. North-Holland, Amsterdam, 2002.

[8] O. FORSTER. *Lectures on Riemann Surfaces (Graduate Texts in Mathematics)*. Springer, 1981.

[9] G. M. GREUEL, CH. LOSSEN, and E. SHUSTIN. *Introduction to Singularities and Deformations*. Springer-Verlag New York Inc., New York, 2007.

[10] G. A. JONES and D. SINGERMAN. *Complex functions: an algebraic and geometric viewpoint*. Press Syndicate of the University of Cambridge, Great Britain, 1987.

[11] E. KUNZ. *Introduction to plane algebraic curves*. Birkhäuser Boston Inc., Boston, MA, 2005. Translated from the 1991 German edition by Richard G. Belshoff.

[12] S. LANG. *Complex Analysis, Fourth Edition*. Springer, New York, USA, 1999.

[13] K. POELKE and K. POLTHIER. Lifted domain coloring. *Computer Graphics Forum*, 28(3):735–742, 2009.

[14] B. POKORNÁ. Quadratic space-like Bézier curves in three dimensional Minkowski space. Project of Dissertation Thesis, 2012.

[15] Python. `http://www.python.org/`, 2012.

[16] C. T. C. WALL. *Singular points of algebraic curves*. Cambridge University Press, New York, 2012.

RNDr. Martina Bátorová, PhD.
Department of Algebra, Geometry and Didactics of Mathematics,
Faculty of Mathematics, Physics and Informatics, Comenius University,
Mlynská dolina, 842 48 Bratislava, Slovakia.
martina.batorova@fmph.uniba.sk

doc. RNDr. Pavel Chalmovianský, PhD.
Department of Algebra, Geometry and Didactics of Mathematics,
Faculty of Mathematics, Physics and Informatics, Comenius University,
Mlynská dolina, 842 48 Bratislava, Slovakia.
pavel.chalmoviansky@fmph.uniba.sk

RNDr. Barbora Pokorná
Department of Algebra, Geometry and Didactics of Mathematics,
Faculty of Mathematics, Physics and Informatics, Comenius University,
Mlynská dolina, 842 48 Bratislava, Slovakia.
barbora.pokorna@fmph.uniba.sk

RNDr. Miroslava Valíková
Department of Algebra, Geometry and Didactics of Mathematics,
Faculty of Mathematics, Physics and Informatics, Comenius University,
Mlynská dolina, 842 48 Bratislava, Slovakia.
miroslava.valikova@fmph.uniba.sk